

Electrodeposition & Characterization of a Corrosion Resistant Zinc-Nickel-Phosphorus Alloy

By A. Krishniyer, M. Ramasubramanian, B.N. Popov & R.E. White

Zinc-nickel-phosphorus alloys were electrodeposited from acid sulfate baths at various current densities and phosphorus levels and were characterized for their corrosion resistance. The corrosion and sacrificial protection abilities of the zinc-nickel and zinc-nickel-phosphorus alloys were tested by chronopotentiometric and linear polarization techniques. Galvanostatic stripping technique was used to determine the qualitative composition of these alloys; the surface morphology and relative composition of the alloys were studied using scanning electron microscopy and energy dispersive X-ray diffraction studies.

Alloys such as Zn-Ni, Zn-Co, Zn-Fe, and Zn-Cd find widespread use in industry as a replacement for direct electroplating of zinc.¹⁻⁴ Among these, the Zn-Ni alloys,⁵ especially with a chromate conversion coating on top, are widely used for corrosion prevention in the automotive plating industry. Zn-Ni alloy with 8–20 percent Ni shows better corrosion resistance compared to pure zinc.⁶ Beyond this level, the alloy can no longer be used to protect substrates such as steel because it becomes more noble and loses its sacrificial protection properties. Moreover, as the alloy corrodes, dissolution of Zn or a Zn-rich phase takes place which would transform the initially less noble, sacrificial character of the alloy into a more noble one than that of the underlying steel. In this event, the substrate steel begins to protect, sacrificially, the covering Zn-Ni alloy.

Several methods have been proposed to improve the corrosion resistance properties of the Zn-Ni alloys without increasing the Ni content. Inclusions of non-metallic elements and compounds such as P,⁹⁻¹³ Al₂O₃,¹⁴ SiO₂¹⁵ etc., have been found to improve the corrosion resistance of various alloy systems. Among these, electrodeposited phosphorus alloys have been found to possess various beneficial proper-

ties, including good magnetic and corrosion resistance characteristics and greater hardness. Swathirajan and Mikhail have studied the corrosion properties of various Ni-Zn-P alloys deposited from a chloride bath. Schlesinger and Meng have demonstrated that it is possible to obtain an electroless thin film deposit of Ni-Zn-P from a chloride bath between pH 8 and 9. Ni-Zn-P alloys obtained by these authors have a lower corrosion rate compared to Zn-Ni alloy. The alloys studied by these authors contain more than 15 percent Ni by weight, however, and so cannot be used to protect steel directly by sacrificial corrosion. Swathirajan and Mikhail have also suggested that multiple layers of Zn-Ni and Ni-P alloys will reduce corrosion rates drastically, compared to a pure Zn or Zn-Ni alloy coating. This alloy sandwich was found to protect steel for a longer time and has a very low corrosion rate. This involves the use of multiple deposition steps and different baths in order to obtain a corrosion resistant Zn-Ni-P alloy.

In this study, electrodeposition of a one-step Zn-Ni-P alloy, which has better corrosion resistance than a comparable Zn-Ni alloy, is proposed. All the alloys studied contain less than 15 percent by weight Ni and can be used as sacrificial coatings for iron. The characterization of zinc-nickel and two different sets of zinc-nickel-phosphorus alloys deposited at various current densities were carried out using chronopotentiometric techniques. The most stable (the rest potential being cathodic with respect to iron for a longer period of time) among these three alloy families were determined and compared with each other. Galvanostatic stripping and linear polarization techniques were used to investigate the reasons for the better stability of the Zn-Ni-P alloy. The surface morphology and the composition of all the alloys were studied using scanning electron microscopy and energy dispersive X-ray diffraction.

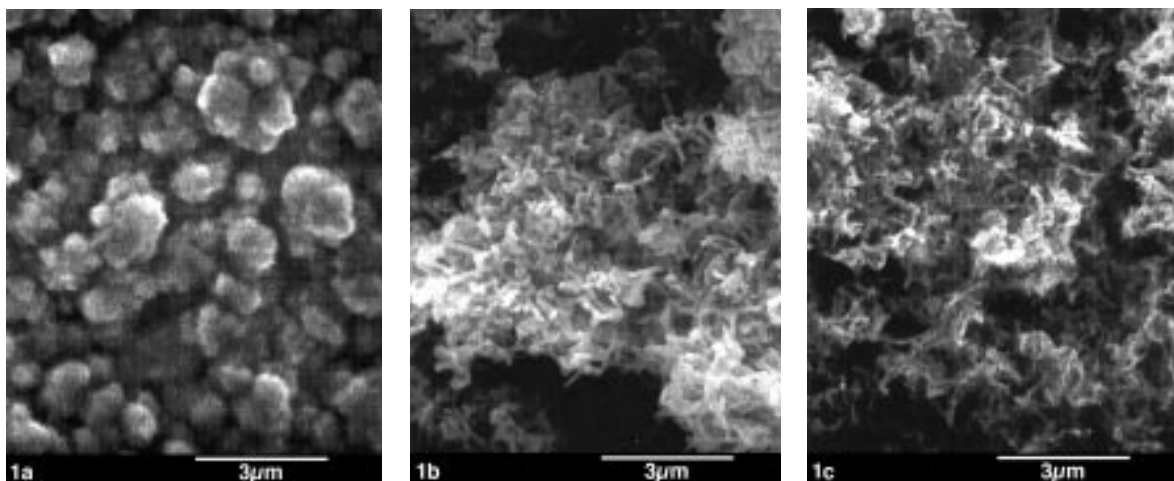


Fig. 1—SEM photomicrograph of (a) Zn-Ni alloy deposited from 0.5 M NiSO₄ + 0.2 M ZnSO₄ + 0.5 M Na₂SO₄ bath at pH 3; (b) Zn-Ni-P (50 g/L) alloy deposited from the same solution + 50 g/L NaH₂PO₂ at pH 3; (c) Zn-Ni-P (100 g/L) alloy deposited from 0.5 M NiSO₄ + 0.2 M ZnSO₄ + 0.5 M Na₂SO₄ + 100 g/L NaH₂PO₂ bath at pH 3. Deposition at current density of 5 mA/cm².

Experimental Procedure

A gold rotating disc electrode with a surface area of 0.458 cm^2 was used as the working electrode for the electrodeposition experiments. A standard calomel electrode was used as the reference electrode and a platinum mesh as the counter-electrode. Zn-Ni alloy deposition was carried out on the rotating disc electrodes at a rotation speed of 1000 rpm, from a bath containing $0.5 \text{ M NiSO}_4 + 0.2 \text{ M ZnSO}_4 + 0.5 \text{ M Na}_2\text{SO}_4$ at a pH of 3.0 ± 0.1 at various current densities. Zn-Ni-P alloys were deposited from two different baths prepared by adding 50 and 100 g/dm^3 of NaH_2PO_2 , respectively, to the above-mentioned Zn-Ni bath. These alloys are designated as Zn-Ni-P (50 g/L) and Zn-Ni-P (100 g/L) alloys, respectively. A potentiostat/galvanostat interfaced with a computer was used during electrodeposition. All depositions were carried out galvanostatically at room temperature in the current density range of $10\text{--}200 \text{ mA/cm}^2$. All solutions were prepared with analytical grade reagents and triply distilled water.

Electrodeposited alloys were immersed in $0.5 \text{ M Na}_2\text{SO}_4 + 0.5 \text{ M H}_3\text{BO}_3$ solution at pH 3.0 and the corrosion potential (E_{corr}) was measured as a function of time. Such tests for the stability of the alloys were carried out for Zn-Ni, Zn-Ni-P (50 g/L), and Zn-Ni-P (100 g/L) alloys deposited at various current densities. During these stability experiments, the electrode was rotated at 300 rpm to minimize the interference of gas bubbles with the corrosion reaction. The most stable alloy among the Zn-Ni, Zn-Ni-P (50 g/L) and Zn-Ni-P (100 g/L) alloys, determined from the previous experiments, was stripped galvanostatically at a current density of 1 mA/cm^2 in $0.5 \text{ M Na}_2\text{SO}_4 + 0.5 \text{ M H}_3\text{BO}_3$ (pH 7) solution. The alloys for this experiment were deposited for a charge equivalent of 4 C. During galvanostatic stripping, the electrode was rotated at 300 rpm as in the previous test.

To characterize the surface structure and to determine the composition of the electrodeposits by SEM/EDX, alloy samples were deposited on iron foils 19.6 cm^2 in area. The baths used for electrodeposition on a rotating disc electrode were also used for deposition of Zn-Ni, Zn-Ni-P (50 g/L) and Zn-Ni-P (100 g/L) on these iron foils. The alloys were deposited galvanostatically at a current density of 5 mA/cm^2 . A special stirring assembly was used to stir the bath at a constant speed of 750 rpm during electrodeposition. The stirrer was held very close to the foil during plating. After

deposition, the samples were washed with distilled water and dried in an oven at $80 \text{ }^\circ\text{C}$ for 10 min. The samples were then analyzed, using SEM and EDX techniques, for surface and alloy characterization.

Results & Discussion

Surface Analysis

Figure 1 shows the surface morphology of Zn-Ni, Zn-Ni-P (50 g/L), Zn-Ni-P (100 g/L) alloys that were deposited on iron foils at a current density of 5 mA/cm^2 . The Zn-Ni alloy morphology consists of large grains, $0.5\text{--}1 \text{ }\mu\text{m}$ in size. The presence of phosphorus in the deposit causes a decrease in the grain size of the alloy. It can be seen that the grain size is small in the Zn-Ni-P (50 g/L) alloy and still smaller and finer in the Zn-Ni-P (100 g/L) alloy. This behavior is typically observed in alloy systems with ternary particles that are known to increase the amorphous character of the deposit. Such increase has also been known to increase the corrosion resistance of the resulting alloys. The compositions of the alloys were obtained by EDX analysis. The average composition of the Zn-Ni alloy was found to be 90 percent Zn and 9.6 percent Ni by weight. The composition of the Zn-Ni-P alloys was found to be 90 percent Zn, 9.4 percent Ni and 0.5 percent P.

Stability Plateaus

Figure 2 shows a plot of the corrosion potential E_{corr} vs. time for the Zn-Ni alloy deposited at three different current densities. These E_{corr} vs. time (stability) tests were carried out in $0.5 \text{ M Na}_2\text{SO}_4 + 0.5 \text{ M H}_3\text{BO}_3$ (pH 3) solution. The alloys were deposited from a $0.5 \text{ M NiSO}_4 + 0.2 \text{ M ZnSO}_4 + 0.5 \text{ M Na}_2\text{SO}_4$ bath at pH 3 for a charge equivalent of 12.88 C. It can be observed from these potential-time plots that there are three distinct plateaus at three different potential values occurring around -1000 mV , -700 mV and -400 mV .

It has been reported in the literature⁶ that electrodeposited zinc-nickel alloy exhibits three major phases, designated as α , γ , and η phases. The α -phase is a solid solution of zinc in nickel with an equilibrium solubility of 30 percent Zn and with face-centered cubic structure. The γ -phase is an intermediate phase with a composition of $\text{Ni}_3\text{Zn}_{21}$ and body-centered cube crystal structure; the η -phase is a solid solution of nickel in zinc with less than one percent nickel and a hexagonal crystal structure. From the composition of these phases and

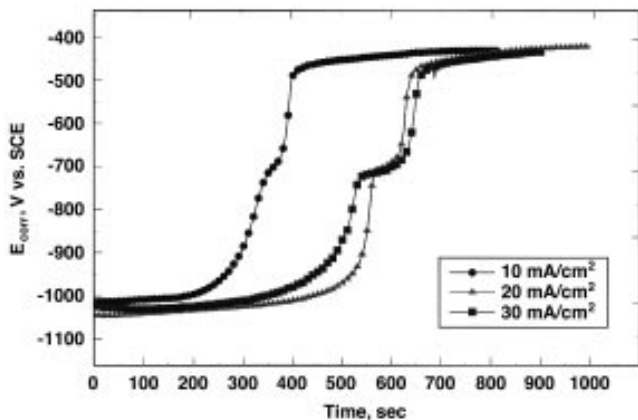


Fig. 2— E_{corr} vs. Time plots for electroplated Zn-Ni alloy immersed in $0.5 \text{ M Na}_2\text{SO}_4 + 0.5 \text{ M H}_3\text{BO}_3$ at pH 3. The Zn-Ni alloys were deposited at various current densities from a $0.5 \text{ M NiSO}_4 + 0.2 \text{ M ZnSO}_4 + 0.5 \text{ M Na}_2\text{SO}_4$ bath at pH 3. Deposition carried out for a charge equivalent of 12.8 C. Rotation speed during deposition: 1000 rpm. Rotation speed during stability test: 300 rpm.

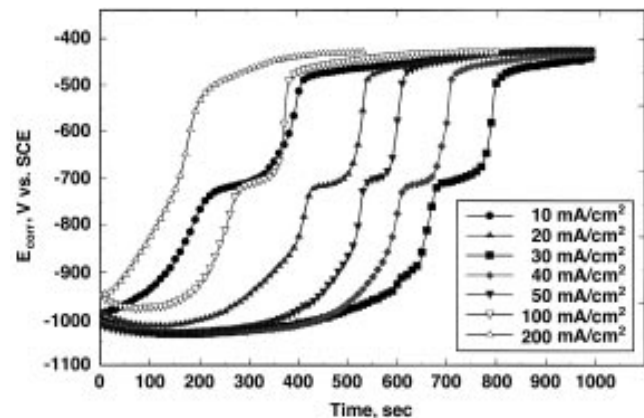


Fig. 3— E_{corr} vs. Time plots for electroplated Zn-Ni-P alloy immersed in $0.5 \text{ M Na}_2\text{SO}_4 + 0.5 \text{ M H}_3\text{BO}_3$ at pH 3. The Zn-Ni-P alloys were deposited at various current densities from a $0.5 \text{ M NiSO}_4 + 0.2 \text{ M ZnSO}_4 + 0.5 \text{ M Na}_2\text{SO}_4 + 100 \text{ g/L NaH}_2\text{PO}_2$ bath at pH 3. Experimental conditions similar to Fig. 2.

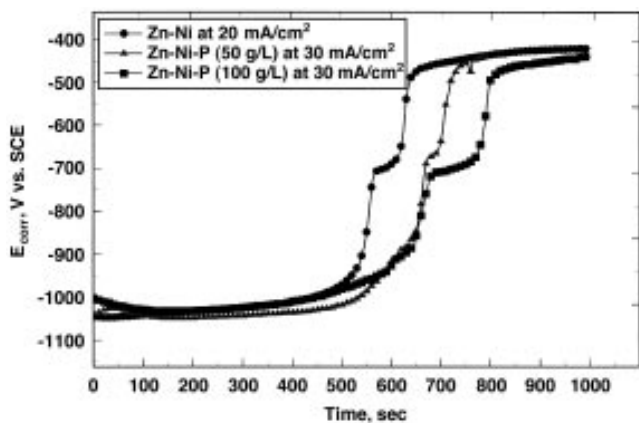


Fig. 4—Comparison of E_{corr} vs. Time plots for electroplated Zn-Ni, Zn-Ni-P (50 g/L) and Zn-Ni-P (100 g/L) alloys immersed in 0.5M Na_2SO_4 + 0.5M H_3BO_3 at pH 3.

their reduction potential available in the literature, it can be said that the plateaus in Fig. 2 are a result of the dissolution of various phases of the alloy. The initial plateau can be assumed to occur because of the dissolution of zinc or a zinc-rich phase (η , δ or γ); the intermediate plateau, resulting from an intermediate zinc phase (β) and the final plateau from a nickel or nickel-rich phase (α).

Figure 2 also shows that the alloy deposited at a current density of 20 mA/cm² (89.5% Zn and 10.3% Ni) is the most stable because it lasts for a longer time under similar corroding conditions. This can be explained by taking into account the kinetics of both zinc and nickel discharge reactions. The zinc-nickel deposition system, like most other anomalous codeposition systems, has a maximum in the zinc content as a function of the deposition current density.¹⁸ According to our previous studies, at very low current densities and under low degrees of cathodic polarization, the main reaction is nickel deposition (under kinetic control) and a parasitic hydrogen evolution reaction. In this region, the potential is insufficient for the less noble metal to deposit; accordingly, the more noble metal (nickel) deposits to a greater extent. With increasing current density, the zinc content in the alloy increases until some intermediate current density where the zinc content is at a maximum. At a current density of 10 mA/cm², the electrodeposition potential was between -1.0 and -1.2 V vs. SCE. This deposition potential is insufficient to deposit necessary quantities of zinc in the alloy. This suggests that the deposit must contain very small amounts of zinc, which explains its rapid dissolution. At a current density of 20 mA/cm², there is sufficient zinc for the alloy to last, in or around its rest potential, for a significantly longer time. At current densities higher than 20 mA/cm², the zinc content increases, but so does the hydrogen evolution rate. Consequently, the deposits obtained at higher current densities are inherently more porous. As a result of the increase in porosity, more surface area is exposed to the solution, causing the alloy to be less stable than those obtained at 20 mA/cm². Deposits obtained at still higher current densities than 30 mA/cm² were also tested, but their stability progressively decreased with increase in current density.

Figure 3 shows the plots of the corrosion potential E_{corr} vs. time for the Zn-Ni-P (100 g/L) alloys at various current densities. The plots show three plateaus corresponding to zinc dissolution from different phases, similar to that of the Zn-Ni alloy. The graph also shows that the stability of the

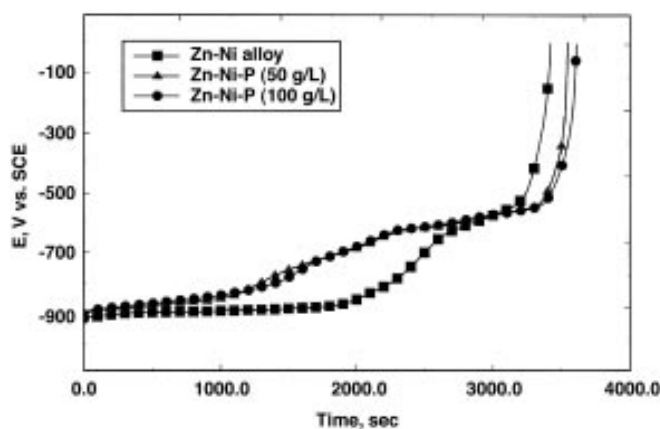


Fig. 5—Galvanostatic stripping behavior of Zn-Ni, Zn-Ni-P (50 g/L) and Zn-Ni-P (100 g/L) at a stripping current density of 1 mA/cm² in 0.5 M Na_2SO_4 + 0.5 M H_3BO_3 (pH 7) solution.

alloy increases with the increase in the current density, attains a maximum, then decreases. Again, as in the case of the zinc-nickel alloys at lower current densities, the deposition potential is not cathodic enough for a sufficient amount of Zn to deposit and, at higher current densities, the increase in hydrogen evolution causes the deposit to become very porous. It is interesting to note that the major contribution to the increase in stability among this family of Zn-Ni-P (100 g/L) alloys, with the increase in the deposition current density, comes from the zinc-rich plateau. The alloy with maximum stability was observed at a current density of 30 mA/cm². Similar stability experiments were also performed for Zn-Ni-P (50 g/L) alloys and the alloy with maximum stability was obtained at a current density of 30 mA/cm². The current density at which the maximum stability occurs for the Zn-Ni-P alloys is higher than that of the Zn-Ni alloy (where the best deposit was obtained at 20 mA/cm²). This increase in current density at which a compact deposit is formed can be explained by taking into account the phosphorus reduction reaction. The presence of phosphorus in the bath causes the potential at a given current density to be slightly more anodic during the deposition. Thus, at a given current density the hydrogen evolution rate will be lesser in Zn-Ni-P alloy compared to the Zn-Ni alloy, and the porosity effects will arise only at even higher current densities. In Fig. 3, a minimum in the corrosion potential can also be observed within 100 sec of the dissolution experiment. This can be explained by the dissolution of a barrier film that has been known to form on zinc in slightly acidic and neutral solutions.

Figure 4 shows the comparison of the E_{corr} vs. time plots between the most stable alloy obtained from Zn-Ni, Zn-Ni (50 g/L) and Zn-Ni-P (100 g/L) baths. It can be noted that the plateaus corresponding to zinc dissolution from the Zn-rich phase in the case of both the Zn-Ni-P alloys are longer. We can also see that the plateau corresponding to the zinc dissolution from the intermediate Zn-Ni phase is longer in the case of the Zn-Ni-P (100 g/L) alloy compared to the Zn-Ni and Zn-Ni-P (50 g/L) alloys. The increase in the zinc dissolution plateau from the Zn-rich phase could be either a result of the increase in the zinc content in this phase or the reduction in the corrosion rate of the Zn-Ni-P alloy. The Zn-Ni-P (100 g/L) alloy also shows a longer zinc dissolution plateau from the intermediate phase of the alloy. The plot also shows the initial rest potentials of both the Zn-Ni-P alloys to be more anodic compared to the Zn-Ni alloy. Because the rest

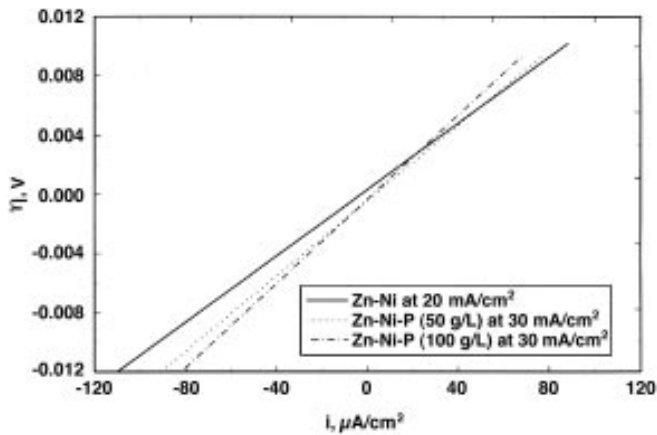


Fig. 6—Linear polarization plots for Zn-Ni, Zn-Ni-P (50 g/L) and Zn-Ni-P (100 g/L) coatings in 0.5M Na₂SO₄ + 0.5M H₃BO₃ at pH 7. The alloys were deposited for an equivalent charge of 8 C. Rotation speed during deposition: 1000 rpm.

potentials of both the Zn-Ni-P alloys were found to be closer to that of the steel substrate when compared to the Zn-Ni alloy, less galvanic corrosion for these alloys can be expected as a result of reduced driving force for corrosion. These observations are confirmed by the results presented in later sections. The stability of these three alloys was also compared in a 0.5 M Na₂SO₄ + 0.5 M H₃BO₃ (pH 7) solution, with similar results.

To determine whether the increase in the stability of the Zn-Ni-P alloys is a result of the increase in Zn content or the decrease in the corrosion rate, galvanostatic stripping experiments were carried out for the three alloys shown in Fig. 4. The alloys were stripped at a current density of 1 mA/cm² in 0.5 M Na₂SO₄ + 0.5 M H₃BO₃ (pH 7) solution. The alloys for this experiment were deposited for a charge equivalent of 4 C. The graph shows two distinct plateaus for each of the three alloys. Again, the potential at which these plateaus occur suggests that they may be construed as resulting from the dissolution of the zinc-rich and nickel-rich phases. We can observe that the plateau corresponding to Zn dissolution from the Zn-rich phase is longer in the case of the Zn-Ni alloy, compared to the Zn-Ni-P alloys. This shows that the Zn content in the Zn-rich phase for the Zn-Ni alloy is greater than in the Zn-Ni-P alloys. Thus, by comparing Figs. 4 and 5, it can be seen that even though the zinc content in the zinc rich-phase is less in the case of the Zn-Ni-P alloys, their stability in the solution is much higher. Accordingly, this points toward an increase in the corrosion resistance as the main reason for the increased stability of the Zn-Ni-P alloys. Figure 5 shows two plateaus at -0.92 V and 0.6 V and a transition region between the two for Zn-Ni alloy. This is in agreement with results reported in the literature.

Corrosion Rate Measurement

The corrosion rate of the coating was measured by linear polarization technique at a scan rate of 0.5 mV/sec in 0.5 M Na₂SO₄ + 0.5 M H₃BO₃ (pH 7) solution. In this experiment, the alloys were allowed to attain a stable rest potential in the same solution before carrying out the linear polarization test. The resulting graphs of overpotential vs. current density are shown in Fig. 6. The slope of these lines yields the value of the polarization resistance. The polarization resistance, obtained from the slope of these graphs in Fig. 6, for the Zn-Ni alloy, is seen to be at minimum and that for the Zn-Ni-P (100

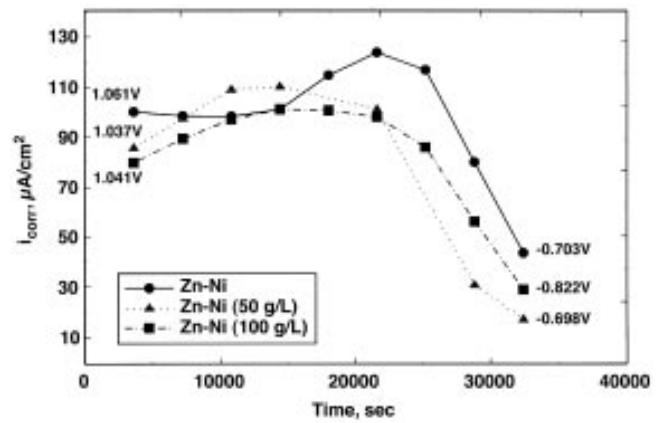


Fig. 7—Plot of corrosion current vs. time for Zn-Ni, Zn-Ni-P (50 g/L) and Zn-Ni-P (100 g/L) coatings in 0.5M Na₂SO₄ + 0.5M H₃BO₃ at pH 7. Rotation speed during deposition: 1000 rpm.

g/L) alloy is maximum. The corrosion current/rate was then calculated using the Stern-Geary equation.

Figure 7 shows the plot of the corrosion current as a function of time for the three alloy deposits. To measure the corrosion current, linear polarization tests were carried out and the polarization resistance was determined at the end of every hour, while the corrosion potential was monitored continuously as a function of time. The corrosion current for the Zn-Ni alloy is greater than both the Zn-Ni-P alloys for almost the entire period of time. It can also be seen that the corrosion rate for the Zn-Ni-P alloys initially increases, then decreases. This can be explained by taking into account the barrier film that is formed on the surface of the alloy. As the barrier film breaks, more and more of the zinc-rich phase of the alloy is exposed to the solution and, as a result, the corrosion rate increases. The corrosion rate attains a maximum when the entire barrier film has been dissolved, and the whole alloy surface is exposed.

Subsequent dissolution of the zinc or zinc-rich phase causes the corrosion rate to decrease because of two factors. The first factor is that the rest potential of the alloy at that time is more anodic than the value with which the alloy started, causing a decrease in the galvanic driving force for corrosion. The second factor is that the dissolution of zinc causes the alloy to become rich in nickel near the surface, which is inherently more corrosion-resistant. In the case of the Zn-Ni alloy, the corrosion rate remains constant for about 15,000 sec, increases, attains a maximum, then decreases. This behavior can also be attributed to the presence of the barrier film on the alloy surface. As in the case of the Zn-Ni-P alloys, the corrosion rate increases when the barrier film dissolves, attains a maximum, then decreases. The decrease in the corrosion rate is a result of the gradual dissolution of zinc, causing the alloy to become nickel-rich near the surface and, consequently, more corrosion-resistant. It can also be seen that at the end of 32,500 sec, the corrosion potential of the Zn-Ni-P (100 g/L) alloy is -0.822 V and that of Zn-Ni, and Zn-Ni-P (50 g/L) alloy are -0.703 V and -0.698 V vs. SCE, respectively. Thus, the Zn-Ni-P (100 g/L) alloy can still protect steel by sacrificial corrosion whereas the Zn-Ni and Zn-Ni-P (50 g/L) alloys cannot.

Findings

A one-step Zn-Ni-P alloy with better corrosion resistant characteristics than a comparable Zn-Ni alloy was devel-

oped. The corrosion resistance and deposition characteristics of two different Zn-Ni-P alloys were compared to Zn-Ni alloy to determine the factors that contribute to the increased corrosion resistance and stability of these alloys. SEM micrographs showed that the grain size of the Zn-Ni-P alloys was much smaller than that of the Zn-Ni alloy. This increase in the amorphous character of the alloy with the increase in phosphorus content could be a major contributing factor for the increased corrosion resistance. The corrosion potentials of the alloys were monitored as a function of time for various current densities of deposition. In all the cases, there existed an optimum current density where the alloy showed maximum stability. The comparison of the stability of the most stable Zn-Ni, Zn-Ni-P (50 g/L) and Zn-Ni-P (100 g/L) alloys showed the Zn-Ni-P (100 g/L) alloy to be the most stable under identical conditions.

The galvanostatic stripping experiments showed that the stability of the Zn-Ni-P (100 g/L) alloy was much higher despite the amount of zinc-rich phase in the alloy's being significantly lower. This suggested that the increased stability arose mainly out of the decreased corrosion rate of the alloys. The results of the corrosion rate experiments showed that the Zn-Ni-P (100 g/L) alloy has a lower corrosion rate compared to the Zn-Ni-P (50 g/L) alloy and Zn-Ni alloy. The rest potentials of the Zn-Ni-P alloys were also found to be more anodic compared to Zn-Ni alloy. This reduces the driving force for the galvanic corrosion of these alloys when used as a protective coating over steel substrates. It was found that the protective barrier film also contributes to the reduction in the corrosion rate initially in the case of the Zn-Ni-P alloys compared to the Zn-Ni alloy. It was also found that the rest potential of the Zn-Ni-P (100 g/L) alloy is cathodic with respect to iron substrates for a longer period of time compared to the Zn-Ni-P (50 g/L) and Zn-Ni alloy and so can serve as a sacrificially protective coating on iron for longer periods of time. Consequently, this new Zn-Ni-P (100 g/L) alloy could be used as an alternative to the Zn-Ni alloy, as a protective coating for iron substrates which could serve as a barrier layer as well as a sacrificially protective coating.

Editor's note: Manuscript received, June 1998.

Acknowledgments

Financial support by AESF, under Research Project RF-93, and A. John Sedriks, of the Office of Naval Research, is gratefully acknowledged.

References

1. D.E. Hall, *Plat. and Surf. Fin.*, **70**, 59 (Nov. 1983).
2. I. Kirilova, I. Ivanov & St. Rashkov, *J. Appl. Electrochem.*, **27**, 1380 (1997).
3. A. Brenner, *Electrodeposition of Alloys*, Vol. II, Academic Press, New York, NY, 1963.
4. K.Kondo, T. Sagawa, & K. Shinohara, *J. Electrochem. Soc.*, **142**, L194 (1995).
5. M.S. Michael, M. Pushpavanam & K. Balakrishnan, *Brit. Corrosion J.*, **30**, 317 (1995).
6. G. Ramesh Babu, G. Devaraj, J. Ayyaparaju & R. Subramanian, *Metal Fin.*, **87**, 9 (1989).
7. B. Lustman, *Trans. Electrochem. Soc.*, **84**, 363 (1943).
8. M. Ramasubramanian, B.N. Popov & R.E. White, *J. Electrochem. Soc.*, in press.
9. S. Swathirajan & Y.M. Mikhail, *ibid.*, **136**, 2189 (1989).
10. M. Schlesinger, X. Meng & D.D. Snyder, *ibid.*, **137**, L1858 (1990).
11. S. Swathirajan & Y.M. Mikhail, U.S. patent 4,758,479 (1988).
12. K. Sridharan, & K. Sheppard, *J. Appl. Electrochem.*, **27**, 1198 (1997).
13. J.L. Carbajal & R.E. White, *J. Electrochem. Soc.*, **135**, 2952 (1988).
14. S. Hashimoto & M. Abe, *Corros. Sci.*, **36**, 2125 (1994).
15. M. Ramasubramanian, PhD thesis, University of South Carolina (1998).
16. S. Swathirajan, *J. Electrochem. Soc.*, **133**, 671 (1986).
17. F. Elkhatabi, M. Sarrat & C. Muller, *J. Electroanal. Chem.*, **404**, 45 (1996).
18. Y.P. Lin & J.R. Selman, *J. Electrochem. Soc.*, **140**, 1299 (1993).
19. B.N. Popov, M. Ramasubramanian, S.N. Popova, R.E. White & K-M. Yin, *J. Chem. Soc., Faraday Trans.*, **92**, 4021 (1996).

About the Authors

Anand Krishniyer is a graduate student in Chemical Engineering at the University of South Carolina. He received his BS degree in electrochemical engineering from the Central Electrochemical Research Institute, Karaikudi, India.

Dr. Murali Ramasubramanian is currently with IBM Corporation, T.J. Watson Research Center, Yorktown Heights, NY. He holds a BS degree from the Central Electrochemical Research Institute, Karaikudi, India. He received his PhD from the University of South Carolina.



Dr. Branko N. Popov* is a research professor at the University of South Carolina, Columbia, SC 29208. He holds a BS degree from the University of Skopje. He received his MS from the University of Illinois, and his PhD from the University of Zagreb.



Dr. Ralph E. White is a professor and department chair in the Chemical Engineering Department at the University of South Carolina. He holds a BS degree from the University of South Carolina. He received his MS and PhD degrees from the University of California at Berkeley.

* To whom correspondence should be addressed.